

# An Optimized FO-PID Controller and Predictive Current Control of the APF Connected AWPS for Power Quality Improvement

**Abstract.** This paper deals with the design of a new topology of arc welding power supply (AWPS) based on an active power filter (APF) suitable to feed an arc welding machine. The principal task of this welding topology is to ensure a good welding process and ensure a unity power factor correction (PF), on the grid side, an active power filter (APF) is connected in parallel between the three-phase full bridge diode rectifier and the grid. The utility of the APF is to provide a unity power factor correction of arc welding power supply (AWPS). The predictive current control (PCC) and self-tuning filter (STF) are used to control the APF. On the arc welding machine side, an optimized FO-PID controller is used to control the welding current and voltage, by controlling the full bridge buck circuit, which offers many exceptional features, like a rapid response to load and grid voltage variations, and inherent short-circuit current limit which results in an improved welding performance and weld bead quality. The performance of the proposed configuration is examined in regards to its power quality given by reading the total harmonic distortion (THD) of the grid current is 3.47%, ensuring the best regulation of the DC-link voltage of APF, and providing a good tuning of the welding voltage and current. The parameters of the FO-PID controller are extracted by a Grey Wolf Optimization approach (GWO). Simulation results are noticed as satisfactory and prove the stability, accuracy, and dynamic response of the synthesized optimized regulating system.

**Streszczenie.** Artykuł dotyczy zaprojektowania nowej topologii zasilania spawarki łukowej (AWPS) opartej na aktywnym filtrze mocy (APF) odpowiednim do zasilania spawarki łukowej. Podstawowym zadaniem tej topologii spawania jest zapewnienie dobrego procesu spawania i zapewnienie jednościowej korekcji współczynnika mocy (PF), po stronie sieci aktywny filtr mocy (APF) jest włączony równolegle pomiędzy trójfazowy prostownik diodowy pełnomostkowy i siatkę. Użyteczność APF polega na zapewnieniu jednościowej korekcji współczynnika mocy zasilacza do spawania łukowej (AWPS). Predykcyjne sterowanie prądem (PCC) i samodostrajający się filtr (STF) służą do sterowania APF. Po stronie spawarki łukowej zoptymalizowany kontroler FO-PID służy do sterowania prądem i napięciem spawania poprzez sterowanie obwodem pełnego mostka buck, który oferuje wiele wyjątkowych funkcji, takich jak szybka reakcja na zmiany obciążenia i napięcia sieci oraz nieodłączne ograniczenie prądu zwarciovego, co skutkuje lepszą wydajnością spawania i jakością spoiny. wydajność proponowanej konfiguracji jest badana pod kątem jakości zasilania podanej przez odczyt całkowitego zniekształcenia harmonicznego (THD) prądu sieciowego wynoszącego 3,47%, co zapewnia najlepszą regulację napięcia obwodu pośredniego APF i zapewnia dobre dostrajanie napięcia i prądu spawania. Parametry regulatora FO-PID są pozyskiwane metodą optymalizacji Gray Wolf (GWO). Wyniki symulacji oceniane są jako zadowalające i świadczą o stabilności, dokładności i dynamicznej odpowiedzi zsyntetyzowanego zoptymalizowanego układu regulacyjnego. (Zoptymalizowany kontroler FO-PID i predykcyjna kontrola prądu podłączonego APF AWPS w celu poprawy jakości energii)

**Keywords:** Arc welding power supply, active power Filter, predictive current control, fractional order PID controller, gray wolf optimization.

**Słowa kluczowe:** zasilanie zgrzewarki, filtr aktywny, sterowanie z prognozą prądu

## Introduction

As welding machines are now being used in many applications even for household purposes without any trained person, it serves a variety of purposes across domains such as machinery and equipment fabricated, structural welding, and offshore welding [1-2], this welding system has to be compact and should have high safety measures. To make the welding system powerful and compact, we necessarily use electronic power converters in the welding machine, to reduce the size of the welding machine [3]. But with the use of power electronic components, there are other problems like harmonics and because of these the power factor of the machine will decrease. For improving the power factor of the arc welding power supply (AWPS), various power factor correction techniques can be used in the literature [4-11]. One is by using passive filters and the other is by using active power filters and others [4]. The active power filter is a converter, which is controlled in such a fashion that the load connected to the converter is seen as an equivalent pure resistance from the source terminals.

The use of an active power filter (APF) to mitigate harmonic problems has drawn much attention because they have excellent compensation characteristics [4]. As a result, the good performance indices have become an important issue to arc welding power supply, they generally first rectify the utility AC power to DC, and then they switch (invert) the DC power into a step-down transformer to produce the desired welding voltage or current. To calculate a justified reference current, a self-tuning filter-based active and

reactive power (STF/PQ) method is used to extract correctly the reference current [12-13].

In this work, we present a novel topology of arc welding power supply (AWPS) based on an active power filter, there are two issues in controlling the proposed welding system. The first issue deals with controlling the welding voltage, in the welding circuit side, an optimized fractional order PID controller (FOPID) is used to control the welding voltage, by consequently generating the switching signal for the signal bridge inverter via the hysteresis current control (HCC). The reason to select the optimized FOPID controller car it increases the degree of freedom and design flexibility of the controller [14-15]. Hence, we chose the Grey Wolf Optimization (GWO) algorithm to select the optimal parameters FO-PID controller.

The second issue, on the grid side, consists of the development of an efficient predictive current control (PCC), which is designed for an active power filtering system in a cooperative with a modified active and reactive power algorithm based on a self-tuning filter. To calculate a justified reference current for such systems, the modified PCC algorithm is considered here as an appropriate technique. The main advantages of this control algorithm are high convergence speed, and robustness concerning load variation [16]. Elsewhere, the advantages of FOPID controllers have good processing [14], which led to the choice of this controller to control the DC-Link capacitor voltage in the APF system to improve the dynamic performance of APF. In this scope, the present work describes how a proposed multi-functional arc welding machine connected active power filter and the grid, can be

achieved, and cooperation of the advantage of all algorithms is illustrated under different operating conditions.

### Configuration of the AWPS based on APF

The power circuit configuration of arc welding power supply incorporating an active power filter is illustrated in Fig.1, the proposed welding system is composed of the main parts, the first one is an active power filter connected between the grid and three phases uncontrolled full bridge rectifier connected at DC-link capacitor voltage  $V_b$  which connected with a single-phase full-bridge buck converter connected. The second part is a high-frequency transformer (HFT) for ensuring high galvanic isolation to supply the welding load, so the welding system is considered a non-linear load, it will inject the harmonic currents and the reactive power at the point of common of the utility, which led to generating the electromagnetic compatibility problem. The main objectives assigned to the proposed system are:

1. Applied the GWO algorithm to select the optimal parameters of the FOPID controller and applied it in the proposed AWPS/APF.
2. Provide a good smooth DC-link capacitor voltage of APF using a FOPID controller.
3. Reach the unity power factor during all operating conditions.
4. Applied the new predictive current control to improve the dynamic performance of the APF.

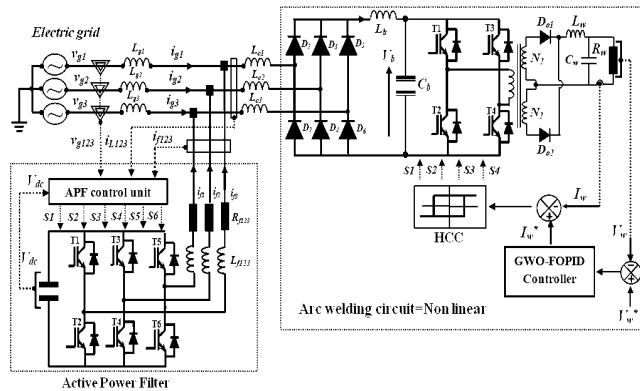


Fig.1. Circuit configuration AWPS-based APF.

### Control Design of the AWPS/APF on the Grid Side

#### A. STF/ PQ algorithm to extract the reference harmonics

In the case where the sources' voltages are distorted, we can use a self-tuning filter with the PQ algorithm [12], the role of the STF is to extract the fundamental components of grid voltage on the axis ( $\alpha$ - $\beta$ ) [13]. So the fundamental components of grid voltage in the axis ( $\alpha$ - $\beta$ ) are the outputs of the STF, which are expressed by (1), (2):

$$(1) \quad v_{g\alpha f} = K \cdot \frac{(s+K)}{(s+K)^2 + \omega_c^2} v_{g\alpha}(s) - \frac{K\omega_c}{(s+K)^2 + \omega_c^2} v_{g\beta}(s)$$

$$(2) \quad v_{g\beta f} = K \frac{\omega_c}{(s+K)^2 + \omega_c^2} v_{g\alpha}(s) + K \frac{(s+K)}{(s+K)^2 + \omega_c^2} v_{g\beta}(s)$$

The three-phase reference filter currents is illustrated by the relation (3).

$$(3) \quad \begin{bmatrix} i_{f1}^* \\ i_{f2}^* \\ i_{f3}^* \end{bmatrix} = \sqrt{\frac{2}{3}} \begin{bmatrix} 1 & 0 \\ -1/2 & \sqrt{3}/2 \\ -1/2 & -\sqrt{3}/2 \end{bmatrix} \begin{bmatrix} i_{f\alpha}^* \\ i_{f\beta}^* \end{bmatrix}$$

The block diagram of the STF-PQ algorithm is illustrated in Fig.2. These references filter current is used in the predictive current control algorithm of APF.

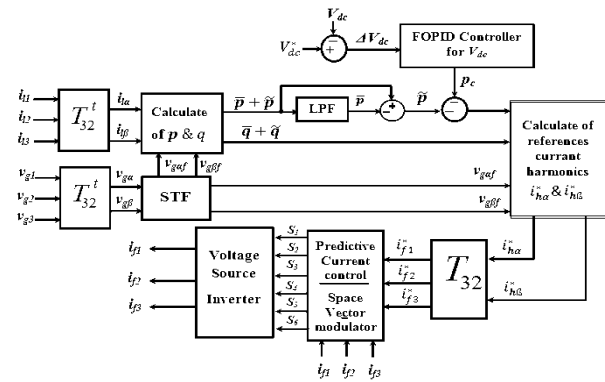


Fig.2. Identification of reference current harmonics by STF/PQ method

#### B. Predictive current control (PCC) for APF current loop regulation

In this part, we present the application of the PCC algorithm for APF along with the reference current generation is carried out. Firstly, it is required to develop a predictive current model of APF to demonstrate this strategy [16]. From the equivalent single-phase circuit of three-phase APF, we can obtain the dynamic model of APF as shown in Fig.1.

$$(4) \quad i_f(k+1) = i_f(k) e^{-\left(R_f/L_f\right)T_s} + \left(E(k) - V_f(k)\right) \left(\frac{1 - e^{-T_s/\tau}}{R_f}\right)$$

The APF current at time instants  $k$  and  $k+1$  are denoted by  $i_f(k)$  and  $i_f(k+1)$ , respectively. And the APF behavior may be then rewritten by (5), and (6), and the detailed predictive current control is described in [16-17].

$$(5) \quad i_f(k+1) = i_f(k) \cdot a + \left(E(k) - V_f(k)\right) \cdot b$$

$$(6) \quad V_f(k+1) = E(k+1) - \frac{1}{b} \left[ i_f^*(k+2) - i_f(k+1) \cdot a \right]$$

The block diagram of overall control is depicted in Fig.3. The results  $V_f(k+1)$  is introduced to the Space Vector Modulator (SVM) block for generating the switching signal of the voltage source inverter of the APF.

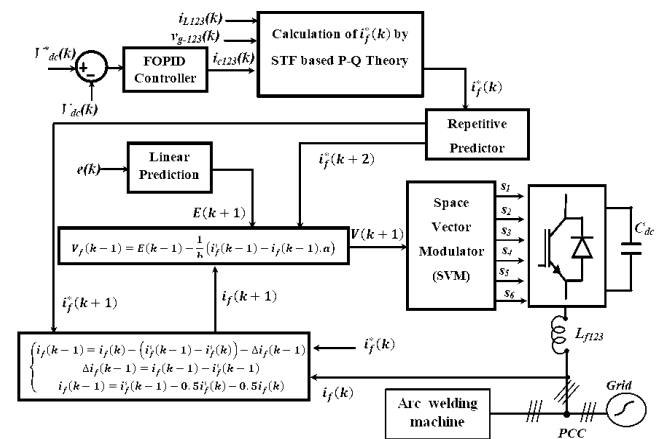


Fig.3. Overall control diagram of the APF system.

## Control Design of the AWPS/APF in Welding Circuit Side

In this part, the main objective of the full bridge back converter (FB-BC) is to step down the welding voltage of AWPS/APF to the desired value using the GWO-FOPID controller. For each switching cycle, the switching pairs  $T_1$ - $T_4$  and  $T_2$ - $T_3$  are turned ON alternately. The operation modes of the full bridge buck converter are the fourth operating modes [5],[8], as illustrated in Fig. 4.

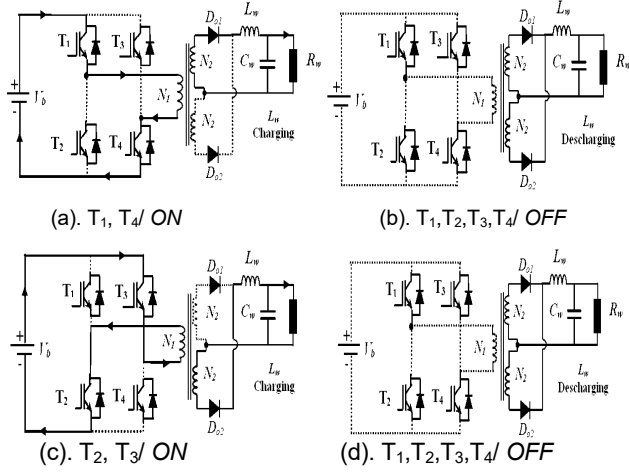


Fig. 4 (a,b,c,d). All operating modes of the FB-BC

### A. Fractional order PID controller

The structure of proposed the fractional order PID controller is depicted in Fig.5. It had the fractional components  $\lambda$  and  $\mu$  in integrator and differentiator respectively [18-19].

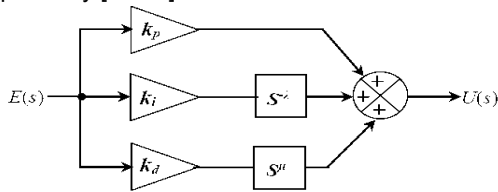


Fig. 5. Structure of fractional-order PID controller

The  $PI^\lambda D^\mu$  control law, to regulate the welding voltage  $V_w$ , in the time domain, is given in (7).

$$(7) \quad u_{FOPID}(t) = k_p e(t) + k_i D_t^{-\lambda} e(t) + k_d D_t^{-\mu} e(t)$$

where  $e(t) = V_w^* - V_w$ . The generalized transfer function of the  $PI^\lambda D^\mu$  is given by (8)

$$(8) \quad G_{FOPID}(t) = k_p + k_i s^{-\lambda} + k_d s^{-\mu}$$

where  $k_p$ ,  $k_i$ , and  $k_d$  are proportional, integral and derivative gains constants respectively,  $\lambda$  and  $\mu$  are fractional order of the integral and derivative term. The term  $s^\lambda$  in (8), has a fractional order that makes it difficult to implement. Hence, the fractional integral operator is approximated using a 5<sup>th</sup>-order O recursive filter [15]. The Oustaloup's approximation of  $s^\lambda$  is given by (9)

$$(9) \quad s^\lambda = \prod_{n=1}^N \frac{1 + \frac{s}{w_{z,n}}}{1 + \frac{s}{w_{p,n}}}$$

The aforementioned approximation is valid for a frequency range between  $[\omega_b; \omega_n]$ . The frequencies of the zeros and poles are evaluated using (10)

$$(10) \quad w_{z,1} = w_b \sqrt{\rho}, \quad w_{p,n} = w_{z,n} \sigma, \quad w_{z,n+1} = w_{p,n} \rho$$

The parameters of this FOPID controller are optimized by using the Grey Wolf Optimization algorithm to regulate the welding voltage.

### B. Grey wolf optimization (GWO) algorithm

The Grey Wolf Optimization (GWO) method is a new heuristic optimization method developed in 2014 by Seyedali Mirjalili [20]. This algorithm mimics the hunting mechanism of grey wolves in the wild [20]. One of the interesting realities of the social life of these wolves is their very strict social hierarchical structure in the group (seen in Figure.6).

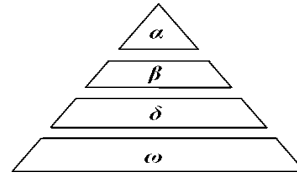


Fig. 6 . Hierarchy of the grey wolf

GWO's hunting strategy and social hierarchy are mathematically modeled to design the GWO optimization algorithm. This algorithm includes the following steps [21-22]:

- Tracking, chasing, and approaching the prey.
- Pursuing, encircling, and harassing the prey until it stops moving
- Attack towards the prey.

The mathematical equations which govern the GWO algorithm can be summarized as follows.

$$(11) \quad D = |CX_p - AX(t)|$$

$$(12) \quad X(t+1) = X_p(t) - AD$$

$$(13) \quad \begin{cases} \vec{X}_1 = X \alpha - A_1 * (D_\alpha) \\ \vec{X}_2 = X \beta - A_2 * (D_\beta) \\ \vec{X}_3 = X \delta - A_3 * (D_\delta) \end{cases}$$

$$(14) \quad X(t+1) = \frac{X_1 + X_2 + X_3}{3}$$

$$(15) \quad A = 2.a.r_1 - a$$

$$(16) \quad C = 2.a.r_2$$

where A, C: Coefficient vectors whose elements are determined randomly. A and C are given by Eq. (15, 16). Also, the components  $\bar{a}$  are linearly decreased from 2 to 0 throughout iterations, and  $r_1$  and  $r_2$  are random vectors in [0, 1].

X: Position vector of the wolf.

$X_p$ : Position vector of the prey.

D: Distance between the positions of the wolf and the prey.

where A and C are the coefficient vectors whose elements are determined randomly. Fig. 7 illustrates the flowchart of the GWO optimization method.

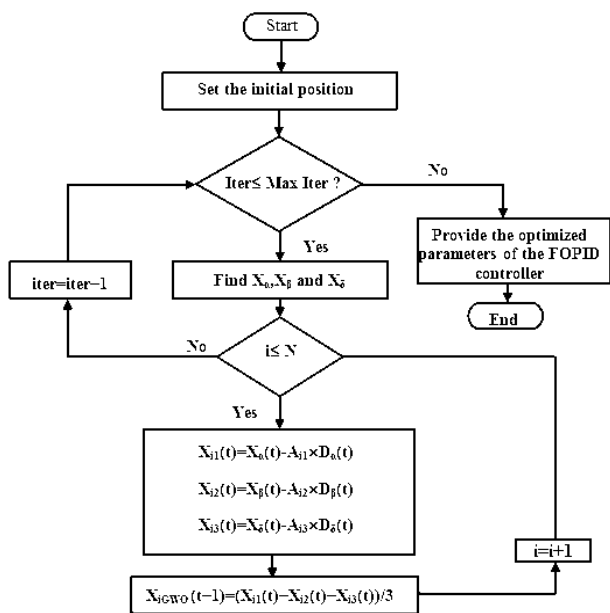


Fig.7.Flowchart of the GWO optimization method

### C. Objective function and constraints of the present work

The integral function of the absolute error multiplied by time (ITAE) is used as an objective function to solve the AWPS problem [15]. The ITAE function is minimized by the GWO strategy. The ITAE performance criterion is calculated by the following expressions:

$$(17) \quad ITAE = J(K_p, K_I, K_D, \lambda, \mu, w_b, w_h) = \int_0^{t_{sim}} t \cdot |e(t)| dt$$

The parameter calibration can be defined by the following formulation, subject to:

$$0.1 \leq K_p \leq 0.2; 250 \leq K_I \leq 350; 150 \leq K_D \leq 300;$$

$$0 \leq \lambda \leq 2; 0 \leq \mu \leq 2; 0.5 \leq w_b \leq 2.5; 0.5 \leq w_h \leq 2.5$$

Minimize:

$$(18) \quad J(x) : x = (K_p, K_I, K_D, \lambda, \mu, w_b, w_h) \in \mathbb{R}^7$$

The GWO parameters are chosen as the total number of iteration  $N_{iter}=50$ , and the search agents number is 10, respectively. The fitness value-iteration curve from GWO tuned FOPID controller is illustrated in Fig. 8.

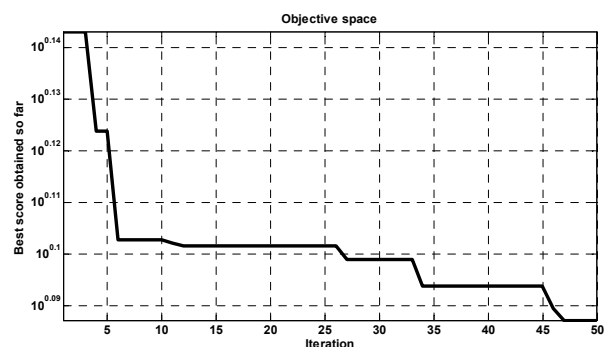


Fig.8. GWO-tuned convergence plots of the cost function

The GWO algorithm provides minimum cost function value and rapid convergence. The general proposed control

scheme for regulating the welding voltage  $V_w$  of a full bridge buck converter is illustrated in Fig. 9.

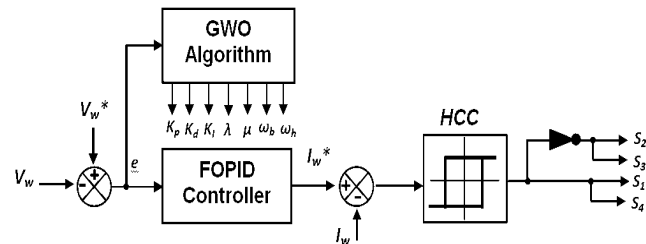


Fig.9. Block diagram of the control scheme for FB-BC.

### Simulation results

The proposed configuration of AWPS with GWO-FOPID controller is simulated in MATLAB/Simulink environment, this proposed configuration and control scheme is simulated and evaluated under constant load conditions and load variation.

The design of the passive circuit of APF is mentioned in [16], also the design of the welding circuit is given in [8] and the specifications for APF-based AWPS are given in Table.1. The parameters of the GWO-FOPID controller, FOPID controller, and the PID controller are given Table.2.

Table 1. Simulation parameter of the proposed AWPS

Grid and APF parameters	welding load parameters
$R_g=1\Omega$ , $L_g=0.15mH$ , $f_g=50Hz$ , $v_g=220V$ , $R_l=1\Omega$ , $L=4.3mH$ , $C_{dc}=3000\mu F$ , $f_s=20kHz$ , $T_s=10\mu s$	$R_c=1\Omega$ , $L_c=4.3mH$ , $L_w=8\mu H$ , $C_w=4\mu H$ , $R_w=0.2\Omega$ , $V_w=20V$ , $C_b=1100\mu F$ , $L_b=1mH$ , $\Delta h=0.01A$ , $f_{FBC}=50kHz$

Table 2. Proposed AWPS controller parameters

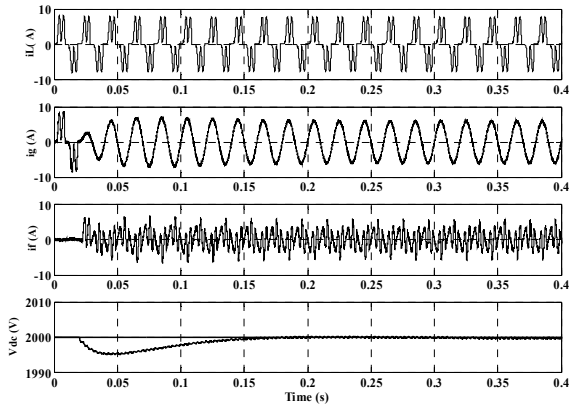
Controller	Welding voltage Controller $V_w$	DC-Linkvoltage Controller $V_{dc}$
GWO-FOPID	$K_p=0.1286651$ ; $K_I=350$ ; $K_D=226.6744$ ; $\lambda=0.2557118$ ; $\mu=0.7132358$ ; $w_b=2.5$ ; $w_h=2.404494$	(FOPID1) $K_{p1}=0.4$ ; $K_{i1}=120.18$ ; $K_{D1}=1.5$ ; $\lambda 1=10.2877$ ; $\mu 1=0.0986$ ; $w_{b1}=2.23$ ; $w_{h1}=2.23$
FOPID	$K_p=1$ ; $K_I=500.18$ ; $K_D=10.8811$ ; $\lambda=0.02877$ ; $\mu=0.986$ ; $w_b=4$ ; $w_h=4$	
PID	$K_p=8.11$ ; $K_I=4.95$ ; $K_D=0.10$	

### A. A steady state of APF-based AWPS

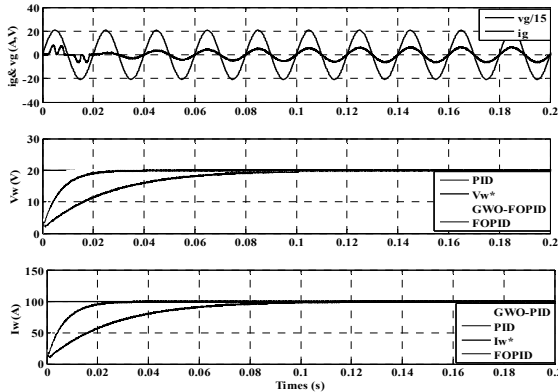
Fig.10 (a, b) shows the steady-state response of the proposed AWPS system, as can be observed, the grid current before filtering is highly distorted during the proceeds of welding, and its THD value is 64,02% (Fig.11.(a)), after switched On the APF the grid current is close to sinusoidal waveform its THD is 3,47%, it meets to IEEE-519 standard (Figure.11.b), the grid current ( $i_g$ ) is in phase with the grid which leads a unity PF.

On the other side, the PCC algorithm and STF-PQ algorithm prove their capabilities in the control of the APF. Also, the DC-link voltage  $V_{dc}$  is kept constant around its reference value during operating welding conditions thanks to the FOPID controller (Fig.9.a).

On the other hand, the welding voltage ( $V_w$ ) is constant and reaches rapidly its reference value (20V) by mean of the GWO-FOPID controller, which has a faster response e time (0.01s), and the welding current ( $I_w$ ) is constant at about (100A).

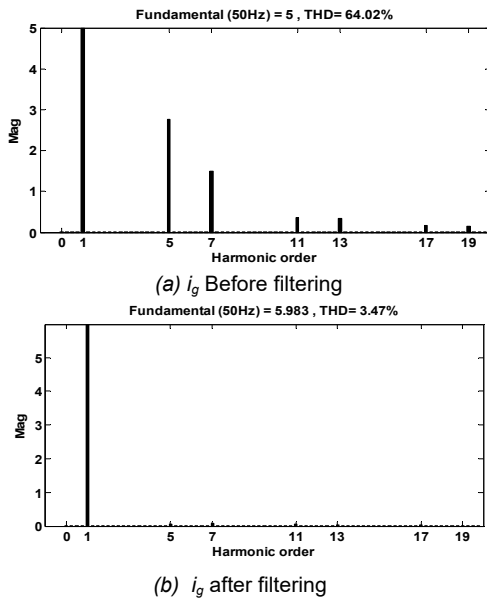


(a). In grid side/APF



(b). In welding circuit side

Fig.10. (a-b). A steady state of the proposed welding system



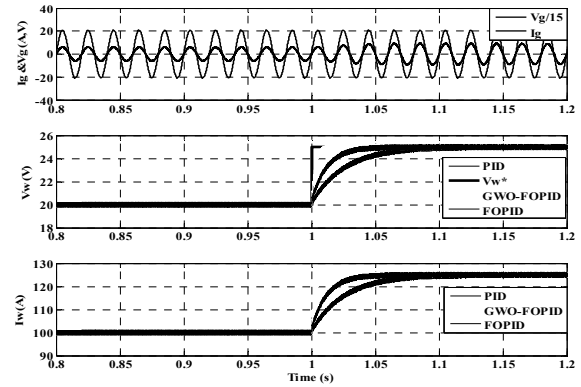
(a)  $i_g$  Before filtering

(b)  $i_g$  after filtering

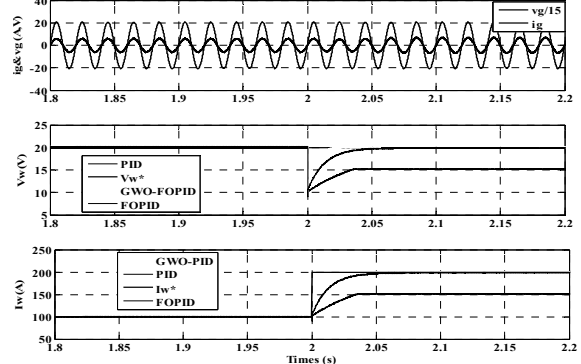
Fig.11 (a-b). THD of grid current after and before filtering

### B. Dynamic performance of the APF-based AWPS

Under a step change of welding voltage ( $V_w$ ) from 20V/25V, excellent tracking performance is reached by using the GWO-FOPID controller. Also in the second test, where we make a step change in resistor load from 0.2Ω/0.1Ω, we observe from Fig.12 that the welding current increases, but with a few fluctuations of welding voltage, the grid current is maintained sinusoidal, and in phase with grid voltage which demonstrate the capability of the proposed PCC control to improve the dynamic response of APF.



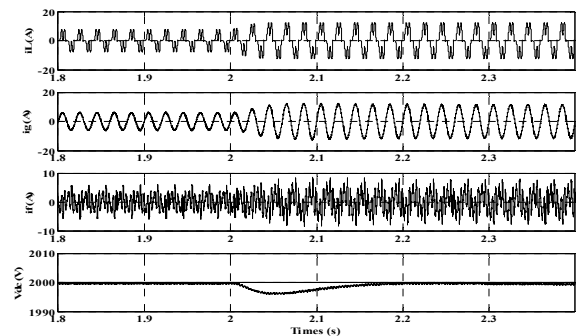
(a). Increase the welding voltage



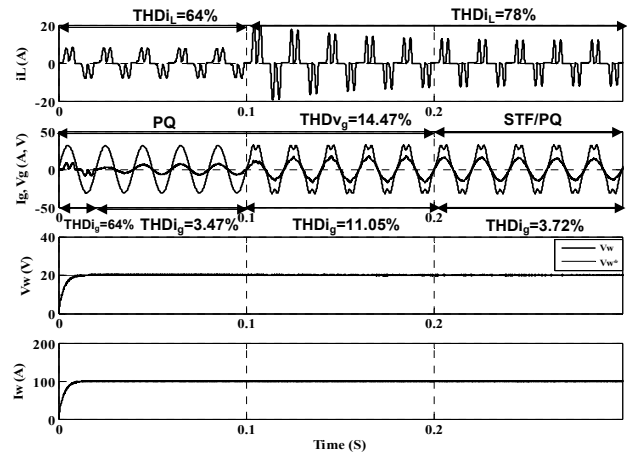
(a). Increase the welding resistor

Fig.12 (a-b). Dynamic performance of the proposed welding system

### C. Dynamic performance of the proposed AWPS under distorted grid voltage



(a). Under step change of welding resistor



(b). Under distorted grid voltage

Fig.13 (a-b). Dynamic performance of the proposed AWPS

Fig. 13 illustrates the good dynamic behavior of the proposed AWPS/APF, where the grid voltage is distorted. We observe at 0.1s that the load current is highly distorted but the grid current is sinusoidal and in phase with the grid voltage, which justifies the capability of the STF/PQ algorithm and the PCC algorithm to improve the dynamic response of AWPS with unity power factor. The welding voltage/current is sties constants 20V and 100A, which proves the robustness of the proposed controller in this operating mode. Fig.13.(a), shows the dynamic response of APF connected arc welding machine, where the welding resistor decreases (0.2 $\Omega$ /0.1 $\Omega$ ), the grid current increases and stays sinusoidal, the DC-link voltage  $V_{dc}$  is fluctuated and reaches its reference value after 0.1s, we can say that FOPID controller is enabled to ensure a constant value of  $V_{dc}$  under step change load, which improve the dynamic performance of APF, the dynamic performance of this AWPS is improved.

## Conclusion

In this article, we have presented a new topology of AWPS and its control schemes. This welding system integrated the functionalities of the APF, which gives its capability to ensure both the weld bead quality, by a good regulation of welding voltage, and at the same time ensure a unity PF by minimizing the THD of the grid current, the advantage guaranteed by the proposed controllers such as the PCC, FOPID and the GWO-FOPID controller for controlling the welding voltage is the major contribution in this work. The system under study was tested by simulation in Matlab/Simulink environment, and the results obtained showed that the grid current was in the same phase with the grid voltage, the THD of the AC main is 3,47%, also a good regulation of the welding voltage, the best robustness, and the faster convergence has been obtained from the GWO-FOPID controller, these performances prove the capability and the effectiveness of this welding topology irrespective of the load variations.

## Acknowledgments

This work was supported by the Research Center in Industrial Technologies (CRTI) and the Directorate General of Scientific Research and Technological development DGRST of Algeria.

**Authors:** PDD. Dr.-Ing. Hamouda Noureddine, Research Center in Industrial Technologies (CRTI), P.O.Box64, Cheraga16014 Algiers, Algeria, [n.hamouda@crti.dz](mailto:n.hamouda@crti.dz), PDD. Dr. Babes Badreddine, Research Center in Industrial Technologies (CRTI), P.O.Box64, Cheraga16014 Algiers, Algeria, [b.babes@crti.dz](mailto:b.babes@crti.dz), PDD. Dr. Kahla Sami, Research Center in Industrial Technologies (CRTI), P.O.Box64, Cheraga16014 Algiers, Algeria, [s.kahla@crti.dz](mailto:s.kahla@crti.dz), Dr. Hamouda Cherif, <sup>2</sup>ALCIOM Company, Yvelines, 3 rue des vignes78220 Yvelines,France, [hamoudacherifdji@gmail.com](mailto:hamoudacherifdji@gmail.com), Dr.-Ing. habil. Rädél Uwe, Fakultät Electrotechnik und informationstechnik, Technisch Universität Ilmenau, Max-Planck-Ring 14, 98693 Ilmenau,Germany, [uwe.radel@tu-ilmenau.de](mailto:uwe.radel@tu-ilmenau.de)

## REFERENCES

- [1] IEC 60974-1., Arc Welding Equipment, Welding power sources, 2005.
- [2] Paul A.K., Power electronics help reduce diversity of arc welding process for optimal performance, in Proc. of Power Electronics, Drives and Energy Systems (PEDES) & 2010 Power India, 2010, 1-7.
- [3] Schupp J., Fischer w., Mecke H., Welding arc control with power electronics, in Proc. Of Power Electronics and Variable Speed Drives, 2000. 443-450.
- [4] Akagi H., Trends in Active Power Line, IEEE Transactions on Power Electronics, 9 (1994), No. 3, 263-268.
- [5] Narula S., Singh B., Bhuvaneshwari G., Improved power quality based welding power supply with Over current handling capability, IEEE Transactions on Power Electronics, 31(2016), No.4, 2850-2859.
- [6] Wang J-M., Wu S-T., Yen S-C., Chiu H-J., A simple inverter for arc welding machines with current doubler rectifier, IEEE Trans Ind Electron, 58(2010), No.5, 278-81.
- [7] Podnebenna, S. K., Burlaka, V. V., Gulakov, S. V., Three-Phase Power Supply For Resistance Welding Machine With Corrected Power Factor, Naukovyi visnyk Natsionalnoho hirnychoho universytetu, 4 (2017), 67-72.
- [8] Narula S., Singh B., Bhuvaneshwari G., Pandey R., Improved power quality bridgeless converter-based SMPS for arc welding, IEEE Transactions on Industrial Electronics,64(2017), No.1, 275-284.
- [9] Wang J-M., S-T Wu., A novel inverter for arc welding machines, IEEE Trans Ind Electron,99(2014), No.1, 1-19.
- [10] Navarro-Crespin. Lopez A., Casanueva V. M., Azcondo F. J., Digital control for an Arc welding machine based on resonant (2013).
- [11] Altanneh N. S., Uslu A., Aydemir, M. T., Design of A Series Resonant Converter GMAW Welding Machine by Using the Harmonic Current Technique for Power Transfer, Electronics, 8 (2019).No.2, 205.
- [12] Czarnecki L.S. , Instantaneous reactive power p-q theory and power properties of three-phase systems, IEEE Transactions on Power Delivery, 21(2006), No. 1, 362-367.
- [13] Birik S., Redif S., Khadem S. k., Basu M., Improved harmonic suppression efficiency of single-phase APFs in distorted distribution systems, International Journal of Electronics, 103(2016), No. 2, 232-246.
- [14] Hamouda N., Babes B., Kahla S., Hamouda C., Boutaghane A., Particle Swarm Optimization of Fuzzy Fractional PD $\mu$ +I Controller of a PMDC Motor for Reliable Operation of Wire-Feeder Units of GMAW Machine, Przegląd Elektrotechniczny, 96(2020), nr 12, 40-46.
- [15] Podlubny I., Fractional order system and PI <sup>$\lambda$</sup> D <sup>$\mu$</sup>  controller, IEEE Transaction on Automatic Control, 44 (1999), No.1, 208-214.
- [16] Hamouda N., Benalla H., Hemsas K., Babes B., Petzoldt J., Ellinger T., Hamouda C., Type-2 Fuzzy Logic Predictive Control of a Grid Connected Wind Power Systems with Integrated Active Power Filter Capabilities, Journal of Power Electronics, 17(2017), No. 6, 1587-1599.
- [17] Hamouda N., Babes B., Kahla S., Soufi Y., Real Time Implementation of Grid Connected Wind Energy Systems: Predictive Current Controller, in Proc. Of The 2019 1st International Conference on Sustainable Renewable Energy Systems and Applications, Algeria, 2019, 1-6
- [18] Babes B., Albalawi F., Hamouda N., Kahla S., Ghoneim S. S. M., Fractional-Fuzzy PID Control Approach of Photovoltaic-Wire Feeder System (PV-WFS): Simulation and HIL-Based Experimental Investigation," in IEEE Access, 9 (2021), 159933-159954
- [19] Hamouda N., Babes B., Kahla S., Beddara A., Aissa O., Boutaghane A., ANFIS Controller Design Using PSO Algorithm for MPPT of Solar PV System Powered Brushless DC Motor Based Wire Feeder Unit, in Proc.Of 2020 International Conference on Electrical Engineering (ICEE) 2020, Istanbul, Turkey.2020,1-6.
- [20] Faris H., Aljarah I., Al-Betar M.A., Mirjalili S., Grey wolf optimizer: a review of recent variants and applications, Neural computing and applications, 30(2018),No. 2, 413-435.
- [21] Mostefai M., Miloudi A., Miloud Y., Parameters Estimation of Photovoltaic Module Using Grey Wolf Optimization Method, Przegląd Elektrotechniczny, 97(2021), nr 2,118-122.
- [22] Dimi-Shahraki M.H., Taghian S., Mirjalili S., An improved grey wolf optimizer for solving engineering problems, Expert Systems with Applications, 166 (2021), No. 1, 113917.